

Ecosystems are showing symptoms of resilience loss

Juan C. Rocha

Stockholm Resilience Centre

Stockholm University

juan.rocha@su.se

Ecosystems around the world are at risk of critical transitions due to increasing anthropogenic pressures and climate change. Yet, it is unclear where the risks are higher or where in the world are ecosystems more vulnerable. Here I measure resilience of primary productivity proxies for marine and terrestrial ecosystems globally. Up to 29% of global terrestrial ecosystem, and 24% marine ones, show symptoms of resilience loss. These symptoms are shown in all biomes, but by large Arctic tundra and boreal forest are the most affected, as well as the Indian Ocean and Easter Pacific. Despite the results are likely an underestimation, they enable the identification of risk areas as well as the potential synchrony of some transitions. Mapping where ecosystems are likely to undergo critical transitions or long transients can help prioritize areas for management interventions and conservation. These results pave the way towards developing an ecological resilience observatory.

Introduction

Ecosystems are prone to non-linear dynamics that can shift their function and structure from one configuration to another.^{1,2} Examples of such regime shifts include the transitions from forest to savannas,³ the collapse of coral reefs,⁴ kelp forest to urchin barrens,⁵ peatland transitions,⁶ or the emergence of hypoxic dead zones in coastal systems.^{7,8} Over 30 different types of regime shifts at the ecosystem scale have been reported in the literature.⁹ Yet predicting when and where they occur remains challenging for most ecosystems.¹⁰ Understanding the answer is deeply related to our ability to observe and measure resilience.

Resilience is the ability of a system to withstand disturbances without losing its function, structure, and hence its identity.^{11–13} A plethora of metrics have been used to approximate resilience, yet the most simple and cross-system indicators used are based on recovery time.^{11,14,15} Time being a common dimension to any dynamical system lends itself for the development of generic proxies of resilience.¹ Complex systems when close to critical transitions leave statistical signatures on the time series of its observables known as *critical slowing down*.^{1,16,17} It means that the system takes longer to recover after a small disturbance, which translates into increases in variance, autocorrelation, and skewness or flickering.^{1,10} Similar indicators exist for spatial data which includes spatial correlations, discrete Fourier transforms, spatial variance, skewness, power spectrums, and patch-size distributions.¹⁸ These methods however have some limitations. They require long time series to detect useful signals,¹⁰ and they can fail when regime shifts are driven by stochastic processes.^{19,20}

Recent theoretical and empirical developments have addressed some of these limitations. On the theoretical front, *critical speeding up* has been proposed as a suitable alternative to detect stochastically driven critical transitions.²¹ While critical slowing down relies on the assumption that resilience loss is driven by a widening and depth loss of the current basin of attraction, critical speeding up assumes that the basin shrinks by narrowing the basin and possibly increasing its depth.²¹ Both techniques pick up resilience loss by measuring changes in the higher moments of the time series distribution by detecting sudden increase (decrease) of variance, autocorrelation, skewness or kurtosis. Another proposed proxy of resilience is the fractal dimension,^{22,23} which is an indication of self-similarity across scales. The fractal dimension is related to how adaptable a system is to perturbations, or how easily it finds modes to deal with disturbances, that has found applications in the diagnosis of cardiac disorders^{22,23} and engineering.²⁴ Exit time has also being proposed as a resilience indicator, it does however requires high resolution long time series with multiple shifts to render useful insights.¹⁵ On

the empirical realm, recent studies have pointed to remote sensing products²⁵ and climate change simulations²⁶ as suitable high dimensional datasets for testing some of these tools in quantifying resilience.

This paper aims to identify where regime shifts are likely to occur by detecting resilience loss in terrestrial and marine ecosystems primary productivity. It applies the traditional early warning signals based on critical slowing down; and adapt the methods to include critical speeding up metrics, and fractal dimension (See Methods). To that end, **gross primary productivity**, terrestrial ecosystem respiration, and **chlorophyll-a concentration** were used as proxies of primary productivity of marine and terrestrial ecosystems. These variables have been harmonized by the **Earth System Data Lab**, meaning that all data layers share the same time (weekly) and spatial (0.25 degree) resolution.²⁷ To quantify and compare the change in resilience indicators, the absolute difference between the maximum and minimum values per indicator was used (Δ , Fig S1), and a segmented regression was used to detect changes in slope and break points in the time series (Methods). A series of logistic and random forests regressions were used to gain insights on what is driving resilience loss in ecosystems world wide.

Results

A

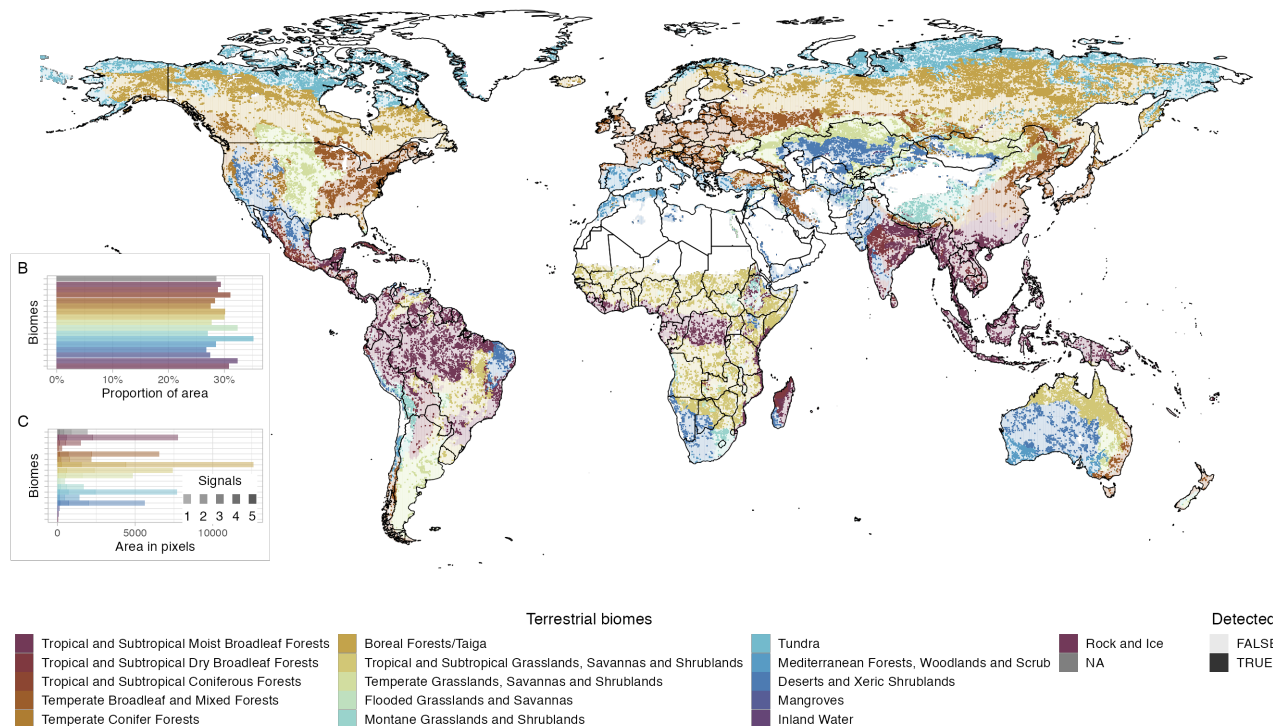


Figure 1: Resilience loss in terrestrial biomes Resilience loss for gross primary productivity is approximated as large differences in standard deviation, autocorrelation at lag-1, skewness, kurtosis or fractal dimension. Differences are considered a symptom of resilience loss if they are above the 95% or below 5% percentiles of the distribution. A) shows where are biomes showing symptoms of resilience loss, B) aggregates proportion of area per biome, while C) shows area in 0.25 degree pixels. A similar figure for terrestrial ecosystem respiration is available in Fig S2. Fig S3 provides maps for each resilience indicator on the gross primary productivity data, and Fig S4 on terrestrial ecosystem respiration.

Ecosystems world wide are showing symptoms of resilience loss. The absolute difference in resilience indicators (Δ) emphasizes jumps on the time series and enables comparison with normal variation adjusted to each biome type. Arctic ecosystems such as boreal forests, taiga and tundra show the strongest signals of resilience loss

globally (Fig 1, S2). However, the extremes of the distributions (5% and 95% percentiles) of each resilience proxy reveals that all ecosystems are losing resilience, for some of them up to 30% of their global area on the gross primary productivity or terrestrial ecosystem respiration data sets (Fig S3, S4).

Despite data incompleteness for marine ecosystems at high latitudes, some signals of resilience loss are detected in Arctic marine systems and the Southern Ocean (Fig 2, S5). The Easter Indo-Pacific, and Tropical Easter Pacific Oceans are the marine biomes with larger areas showing symptoms of resilience loss (Fig 2). The high oceans, however, show by far the larger areas affected with hot spots outside the Caribbean basin in the Tropical Atlantic, the Tropical Pacific and south west Madagascar.

Symptoms of resilience loss are coherent in space and time. Despite the analysis was done independently for each time series and variable, spatial aggregation and coincidence of break points in time suggest that the signals are not an artifacts of the data used (Fig S6, S7, S8). On the contrary, it supports the idea that there are edges in the three-dimensional space (longitude, latitude and time) that enclose volumes whose dynamics can shift in tandem.²⁶ Resilience indicators are remarkably consistent across metrics for marine systems both in space (Fig S5) and time (Fig S8). There is high agreement between kurtosis and skewness across all data sets (Figs S3, S4, S5), they can signal possible shifting of basin of attraction or dynamic transients.^{1,10}

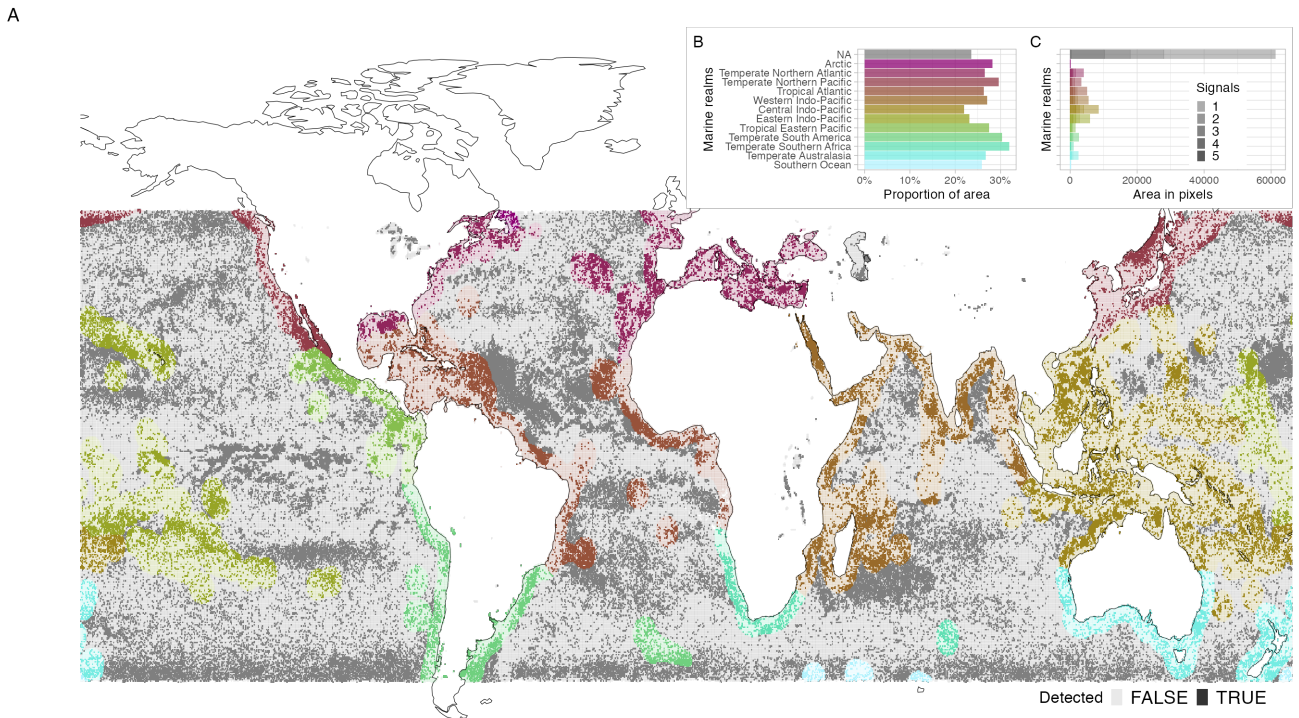


Figure 2: Resilience loss in marine realms Detection of resilience loss using chlorophyll-A as proxy of primary productivity (A). B) aggregates proportion of area per realm, while C) shows areas in 0.25 degree pixels. Maps for each resilience indicator are provided in Fig S5

Signals of resilience loss, however, do not conform neatly with slowing down or speeding up theories. Only a minority of places show consistent increase or decrease in variance and autocorrelation (Fig S3, S4, S5). Lack of consistency between signals suggests that there is no one preferred theory at place. But instead, multiple drivers are interacting in pushing ecosystems outside their realm of stability, some of them through increasing stochasticity while others through slow forcing. To test that hypothesis, I used a logistic regression and a random forests to investigate what is driving the detection of early warnings. Detection by at least two proxies of resilience loss was used as response variable. Explanatory variables for terrestrial ecosystems

included time series of temperature, precipitation, burned area, and land cover. For marine systems, the explanatory variables were restricted to sea surface temperature and sea surface salinity. Variables with long and frequent time series (temperature, salinity and precipitation) were filtered with a Fourier transform to test whether the signals are predicted by long term variation, annual cycles, fast oscillations or the linear (slow) trends. All regressions used a stratified sampling design, balanced on detection, and with fixed effects per biomes or marine realm respectively (See Method).

The strongest predictors of resilience loss are indeed a combination of slow forcing and stochasticity in environmental variables such as temperature, precipitation, or sea surface salinity. For terrestrial biomes, mean temperature, mean precipitation and variability in fast oscillations and annual cycles are the strongest predictors, while marine realms are predicted by mean temperature, mean salinity and their variability at different time scales (Fig S9). The logistic regression facilitates a relative straight forward interpretation.²⁸ Once geography and biome type has been controlled for, the reminder coefficients indicate what increases the odds of detecting resilience loss. However, this linear approach suffers from correlations in the predictors, namely the different time scales at which the hypothesis needs to be tested, whether it is slow forcing or stochasticity in different time scales what drives the signals. In fact, the predicting accuracy for the logistic regression is poor (area under the receiver operating characteristic curve ROC 0.71, 0.65 and 0.59 for gross primary productivity, terrestrial ecosystem respiration and chlorophyll A respectively). The random forest approach render a higher predictive power (ROC 0.893, 0.874, 0.827 respectively). It is robust to potential correlations and required less pre-processing for feature engineering, but is less amenable for interpretation.²⁸ It reveals which variables improve predictions but not necessarily in which direction they are affecting resilience loss. The results of both approaches confirm the hypothesis that resilience loss is driven by a combination of slow forcing and stochasticity on potential drivers.

Discussion

Globally 29% of terrestrial biomes and 24% of marine realms show some signals of resilience loss. The overall patterns here reported agree with recent reports documenting ecosystem's degradation worldwide. Forests are becoming more vulnerable to droughts, and the combined effects with increasing fire frequency are exposing them to major diebacks expected by mid-century.²⁹ Temperature thresholds for terrestrial primary productivity have been identified^{30,31} where carbon uptake is potentially degraded (sink to source transition). Less than 10% of the terrestrial biosphere has already crossed the threshold, and under business as usual scenarios, half of the biosphere is expected to cross these thresholds by the end of the century, with the most affected areas being Canadian and Russian boreal taigas as well as the Amazon and South East Asia rainforest.³⁰ These are biomes where strongest signals of resilience loss were detected. Other studies quantifying terrestrial ecosystem's resilience with NDVI data also show strong signals from tundra and boreal forests.³²

The marine patterns here presented also align with previous studies. Deepening of the ocean's mixed layer can decrease light conditions near surface, decreasing nutrient exchange in the water column and consequently primary productivity.³³ The area outside the Caribbean basin here reported coincides with an area where salinity has contributed to ocean stratification.³³ Upwelling systems are also hotspots where resilience loss is identified. Upwelling strength is expected to change with climate change, with strengthening already reported in the California and Benguela currents, while weakening in the Iberian-Canary system.³⁴ Upwelling weakening can limit nutrients in marine food webs, while strengthening can over enrich nutrients, and facilitate the onset of oxygen minimum zones.⁷ Our results present an additional line of support that these systems are being destabilized.

The results are limited by the temporal and spatial scale of the available data. If the grain of the data is not frequent enough to match fast dynamics, long enough to capture change in slow processes,^{1,10,15} or the spatial resolution is too coarse, local transitions in space and time can be missed. This is the case with hypoxic areas, where large oxygen minimum zones are identified, but not the diverse range of local cases previously reported.⁷ Only regime shifts that are drastic enough to change primary productivity as observed from remote sensing products can be identified. Regime shifts that impact specific populations or community assemblies without changing primary productivity are missed. Such is the case of coral transitions in the Great Barrier Reef where ~50% of the reef community collapsed following the heatwave events of 2016-17.³⁵

Because of these limitations, the results likely are an under estimation. The estimates are also conservative, with an arbitrary 5% and 95% quantile of the Δ distribution as detection threshold. A lower cutoff would enlarge the areas where resilience loss is detected, but also increase the risk of false positives. A similar study using NDVI data estimated up to ~65% of terrestrial ecosystems show early warning of critical transitions, with strong bias towards boreal forest and taiga.³² The estimates here presented complement previous efforts^{25,32} in taking into consideration fixed effects by biome and a pre-processing technique that removes seasonality and long term variations that can lead to errors, or bias towards high variable environments (higher latitudes).

Despite its limitations, this first-order approximation to resilience loss can help outline priority areas for management. Russia, Canada, the US and Australia are countries with the largest areas of resilience loss identified, yet by proportion of territory, small island states top the ranking. When accounting for the diversity of ecosystems showing signs of resilience loss, megadiverse countries like Brazil, India, Mexico, Indonesia, Australia or Colombia are on the top 10 (Fig S10). Australia has recently been reported as a hotspot for ecological collapses for both marine and terrestrial ecosystems.³⁶ The spatial resolution of the maps here presented enable countries, regions, and even municipalities to update land use planning and take into consideration the vulnerability of their ecosystems. Companies for example, can take such risk into account when deciding on relocation, resource outsourcing, or (d)investments. Countries and municipalities can balance the trade-off between maximizing a particular ecosystem service (e.g. a monoculture) in favour of multifunctional landscapes that include other values such as recreation, spiritual values, or conservation. No matter the scale, we all have a role to play in caring for ecosystems resilience and maintaining their ability to provide the ecosystem services we all depend on.

Future global resilience assessments could benefit from other data streams, particularly other anthropogenic drivers here overlooked. Additional data would however require long time series coverage and high spatial resolution. The accuracy of the predictive models here presented can be improved by using non-linear approaches such as deep neural networks or other machine learning techniques.³⁷ However, these approaches have limited interpretability and often require manually annotated datasets to measure performance. Qualitative efforts such as the Global Ocean Oxygen Network⁷ or the Regime Shifts Database⁹ can provide the annotated examples to train such models. A spatially explicit map of resilience loss can also help quantify the risk of cascading effects in ecosystems previously identified.³⁸ As new Earth observations become available, these global maps can be updated and track how ecosystems resilience is evolving, where are they recovering, and where they become vulnerable. This paper showcases the first steps towards an ecological resilience observatory.

Methods

Data: Gross primary productivity, terrestrial ecosystem respiration (both in $gCm^{-2}d^{-1}$), and chlorophyll-a concentration (mgm^{-3}) were used as proxies of primary productivity of terrestrial and marine ecosystems respectively.³⁹⁻⁴¹ Although these data sets are freely available through the FLUXCOM initiative (<http://www.fluxcom.org>) or the European Space Agency Climate Change initiative (<https://climate.esa.int/>), the versions of the data used here were harmonized by the [Earth System Data Lab](#) to weekly observations at 0.25 degree grid resolution, and stored as [Zarr](#) data cubes to facilitate out of memory computations.²⁷ Gross primary productivity and terrestrial ecosystem respiration time series span the period 2001-2018 resulting in 210 771 terrestrial pixels with 817 time observations each, while chlorophyll A span the period 1998-2018 resulting in 418 776 time series with 966 observations each. The Nature Conservancy classification of terrestrial biomes and ecosystems was used (16 biomes, 812 ecosystems) based on,⁴² while marine realms (N=12) followed⁴³ classification.

Pre-processing: The [Earth System Data Lab](#) is hosted by the Max Planck Institute of Biogeochemistry and Brockmann Consult GmbH with the support of the European Space Agency. Their computing services were used to pre-process the data in their [Julia](#) environment. For each of the resulting time series, missing data was inputted with the mean seasonal cycle. A fast Fourier transform was used to filter the time series and remove the trend, annual cycle, and long-term variability. The remaining fast oscillations were log-transformed and normalized to zero mean and unit variance. The cleaned data was exported and further statistical analysis performed in [R](#). A unit root test showed that a few time series were not stationary after the pre-processing steps described. Thus all time series were first-differenced to remove any remaining seasonality.

Proxies of resilience: At this point all time series are expected to have zero mean and unit variance. Resilience loss is here detected by measuring critical slowing down or speeding up in terms of sharp increase (decrease) of variance measured as standard deviation, autocorrelation coefficient at lag-1; or proxies of flickering such as skewness, and kurtosis. Fractal dimensions were calculated using the madogram method.⁴⁴ All these statistics were calculated in rolling windows half of the size of the time series available. Δ is the difference between maximum and minimum values of the resilience indicators. For standard deviation and autocorrelation at lag-1, a positive Δ can indicate critical slowing down, or speeding up if negative. The value of Δ however is not informative by itself. The magnitude depends on the pre-processing choices. Other researchers prefer a Gaussian filter, or kernel based methods to pre-process time series. These methods, however, require arbitrary choices that can optimize for detection of certain biomes while under estimating for others. Because the data here analyzed span about two decades, care should be taken to avoid bias on the resilience indicator by seasonal variability, annual cycles, or multidecadal oscillations. For these reasons the Fourier transform was an ideal filter for this study, returning zero mean and unit variance fast oscillations regardless whether the time series comes from a strong seasonal biome (e.g. boreal forest) or weak seasonality (e.g. tropical ones). The value of Δ varies, however, with window size, the smaller the rolling window, the larger Δ becomes. What matters, however, is not the absolute value of Δ but its position relative to the distribution for the planet, and in particular, relative to the biome described (due to the seasonality differences). Δ has a bimodal distribution (because zero differences are very unlikely), and outliers with respect to each biome distribution were reported as places showing symptoms of resilience loss. Outliers are here defined as places where Δ is unusually extreme, either above the 95% or below the 5% quantiles of Δ distribution.

To check for the spatial and temporal coherence across time series, a segmented regression⁴⁵ was used to identify the breaking point at which the early warning is detected, and a Davis test for the significant difference in slopes before and after the breaking point. Since the time series are normalized, the expectation is no difference in variance and hence no detection of breaking points. If there is a breaking point and the difference is significant and large, one can expect the signal to be a warning of resilience loss, specially in the case where other neighbouring areas show similar signals in space and time. The statistical detection treats each time series independently, but spatial and temporal coherence of the signal offers supporting evidence for true detection in the absence of annotated data or ground truth.

Regressions: To further explore what is driving resilience loss, a logistic regression and a random forest were fitted to classify pixels where at least two metrics suggested loss of resilience. Explanatory variables included air temperature at 2m (<https://cds.climate.copernicus.eu/cdsapp#!/dataset/ecv-for-climate-change>), sea surface temperature⁴⁶ (<https://climate.esa.int/en/projects/sea-surface-temperature>), precipitation (<https://gpm.nasa.gov/data>), sea surface salinity (<https://climate.esa.int/en/projects/ocean-colour>), burned area (<http://www.globalfiredata.org>), and land cover change (<https://cds.climate.copernicus.eu/cdsapp#!/dataset/satellite-land-cover>). For all variables, except land cover, the available data match the temporal resolution of the data used as proxy of primary productivity, but not necessarily time span. Thus, a Fourier transform was used to pre-process the data and separate the linear trend, seasonal cycle, annual cycle and fast oscillations. For temperature, precipitation, and salinity, their mean value, slope of the linear trend, and the standard deviation of the seasonal cycle, annual cycle and fast oscillations were used as regressors. This is with the intention of testing whether resilience loss is driven by variability at different time scales or changes in slow processes. Land cover data has a higher spatial resolution (300m) but lower temporal resolution (year). Proportion of change per land cover class between 1994 and 2018 were calculated and aggregated at 0.25 degree grid. Burnt area is the aggregated area burned in hectares during 2001-2018 per pixel.

For logistic regressions, the data was down sampled on the detection variable (at least two variables indicating resilience loss), after filtering out rock and ice biomes, log-transforming burnt area, performing a box-cox transformation on land cover change variables, and normalizing to zero mean and unit variance all numeric predictors. Random forest, being more tolerant to variables on their natural units, were fitted after filtering out rock and ice biomes and down sampling on detection. 75% of the data was used for training and tuning hyper parameters using 10-fold cross validation. All random forest were fitted with 1000 trees. Best models were assessed against the testing data (25%) and variable importance computed with permutation. The best model for gross primary productivity targeted node size 10 and 12 variables to split at each node (N = 31122, OOB error 0.13), 20 node size and 9 variables for terrestrial ecosystem respiration (N = 29546, OOB error 0.14), and 20 node size and 9 variables for chlorophyll A (N = 54298, OOB error 0.16).

Data availability: All data used in this study is publicly available through the Copernicus Climate Change and Atmosphere Monitoring Service, NASA, FLUXCOM initiative, or the Global fire emissions database. Links to each data set are provided when introduced under the section data or regressions.

Computer code: All code used in this analysis is available at <https://github.com/juanrocha/ESDL>

Acknowledgements

This work would have not been possible without the open data provided by Copernicus Climate Change and Atmosphere Monitoring Service, NASA, FLUXCOM initiative, and the Global fire emissions database. JCR would like to thank the European Space Agency and the Max Planck Institute of Biogeochemistry for an early adopter grant to use the Earth System Data Lab curated data sets and computational facilities. JCR was also supported by Formas grants 942-2015-731, 2020-00198 and 2019-02316, the latter through the Belmont Forum.

References

1. Scheffer, M. *et al.* Early-warning signals for critical transitions. *Nature* **461**, 53–59 (2009).
2. Folke, C. *et al.* Regime shifts, resilience, and biodiversity in ecosystem management. *Annu Rev Ecol Evol S* **35**, 557–581 (2004).
3. Hirota, M., Holmgren, M., Nes, E. H. van & Scheffer, M. Global resilience of tropical forest and savanna to critical transitions. *Science* **334**, 232–235 (2011).
4. Hughes, T. P. *et al.* Coral reefs in the Anthropocene. *Nature* **546**, 82–90 (2017).
5. Ling, S. D. *et al.* Global regime shift dynamics of catastrophic sea urchin overgrazing. *Philos. Trans. R. Soc. Lond., B, Biol. Sci.* **370**, 20130269–20130269 (2015).
6. Turetsky, M. R. *et al.* Global vulnerability of peatlands to fire and carbon loss. *Nature Geoscience* **8**, 11–14 (2015).
7. Breitburg, D. *et al.* Declining oxygen in the global ocean and coastal waters. *Science* **359**, eaam7240 (2018).
8. Díaz, R. J. & Rosenberg, R. Spreading Dead Zones and Consequences for Marine Ecosystems. *Science* **321**, 926–929 (2008).
9. Biggs, R., Peterson, G. & Rocha, J. The Regime Shifts Database: a framework for analyzing regime shifts in social-ecological systems. *Ecology and Society* **23**, art9 (2018).
10. Dakos, V., Carpenter, S. R., Nes, E. H. van & Scheffer, M. Resilience indicators: prospects and limitations for early warnings of regime shifts. *Philos. Trans. R. Soc. Lond., B, Biol. Sci.* **370**, 20130263–20130263 (2015).
11. Holling, C. S. Resilience and stability of ecological systems. *Annual review of ecology and systematics* **4**, 1–23 (1973).
12. Folke, C. Resilience (Republished). *Ecology and Society* **21**, art44 (2016).
13. Gao, J., Barzel, B. & Barabasi, A.-L. Universal resilience patterns in complex networks. *Nature* **530**, 307–312 (2016).

14. Scheffer, M. *Critical Transitions in Nature and Society*. (Princeton University Press, 2009).
15. Arani, B. M. S., Carpenter, S. R., Lahti, L., Nes, E. H. van & Scheffer, M. Exit time as a measure of ecological resilience. *Science* **372**, (2021).
16. Strogatz, S. H. *Nonlinear Dynamics and Chaos*. (Hachette UK, 2014).
17. Scheffer, M. *et al.* Anticipating Critical Transitions. *Science* **338**, 344–348 (2012).
18. Kéfi, S. *et al.* Early Warning Signals of Ecological Transitions: Methods for Spatial Patterns. *PLoS ONE* **9**, e92097 (2014).
19. Hastings, A. *et al.* Transient phenomena in ecology. *Science* **361**, eaat6412 (2018).
20. Hastings, A. & Wysham, D. B. Regime shifts in ecological systems can occur with no warning. *Ecol. Lett.* **13**, 464–472 (2010).
21. Titus, M. & Watson, J. Critical speeding up as an early warning signal of stochastic regime shifts. *Theor. Ecol.* **280**, 20131372 (2020).
22. West, G. *Scale*. (Penguin, 2017).
23. West, B. J. Fractal physiology and the fractional calculus: a perspective. *Front. Physiol.* **1**, (2010).
24. Pavithran, I. & Sujith, R. I. Effect of rate of change of parameter on early warning signals for critical transitions. 013116 (2021).
25. Verbesselt, J. *et al.* Remotely sensed resilience of tropical forests. *Nature Climate Change* **6**, 1028–1031 (2016).
26. Bathiany, S., Hidding, J. & Scheffer, M. Edge Detection Reveals Abrupt and Extreme Climate Events. *J. Climate* **33**, 6399–6421 (2020).
27. Mahecha, M. D. *et al.* Earth system data cubes unravel global multivariate dynamics. *Earth System Dynamics* **11**, 201–234 (2020).
28. Kuhn, M. & Johnson, K. *Applied Predictive Modeling*. (Springer Science & Business Media, 2013).
29. Williams, A. P., Allen, C. D., Macalady, A. K. & Griffin, D. Temperature as a potent driver of regional forest drought stress and tree mortality. *CommsEnv* **3**, (2013).
30. Duffy, K. A. *et al.* How close are we to the temperature tipping point of the terrestrial biosphere? *Science Advances* **7**, eaay1052 (2021).
31. Johnston, A. S. A. *et al.* Temperature thresholds of ecosystem respiration at a global scale. *Nature Ecology & Evolution* **5**, 487–494 (2021).
32. Feng, Y. *et al.* Reduced resilience of terrestrial ecosystems locally is not reflected on a global scale. *CommsEnv* **2**, (2021).
33. Sallée, J.-B. *et al.* Summertime increases in upper-ocean stratification and mixed-layer depth. *Nature* **591**, 592–598 (2021).

34. Sydeman, W. J. *et al.* Climate change. Climate change and wind intensification in coastal upwelling ecosystems. *Science* **345**, 77–80 (2014).
35. Hughes, T. P. *et al.* Global warming transforms coral reef assemblages. *Nature* **556**, 492–496 (2018).
36. Bergstrom, D. M. *et al.* Combating ecosystem collapse from the tropics to the Antarctic. *Glob Change Biol* **27**, 1692–1703 (2021).
37. Reichstein, M. *et al.* Deep learning and process understanding for data-driven Earth system science. *Nature* **566**, 195–204 (2019).
38. Rocha, J. C., Peterson, G., Bodin, O. & Levin, S. Cascading regime shifts within and across scales. *Science* **362**, 1379–1383 (2018).
39. Jung, M. *et al.* The FLUXCOM ensemble of global land-atmosphere energy fluxes. *Scientific Data* **6**, 74 (2019).
40. Tramontana, G. *et al.* Predicting carbon dioxide and energy fluxes across global FLUXNET sites with regression algorithms. *BIOGEOSCIENCES* **13**, 4291–4313 (2016).
41. Sathyendranath, S. *et al.* An Ocean-Colour Time Series for Use in Climate Studies: The Experience of the Ocean-Colour Climate Change Initiative (OC-CCI). *Sensors (Basel)* **19**, (2019).
42. Olson, D. M. *et al.* Terrestrial Ecoregions of the World: A New Map of Life on Earth. *BioScience* **51**, 933 (2001).
43. Spalding, M. D. *et al.* Marine Ecoregions of the World: A Bioregionalization of Coastal and Shelf Areas. *BioScience* **57**, 573–583 (2007).
44. Gneiting, T., Ševčíková, H. & Percival, D. Estimators of fractal dimension: Assessing the roughness of time series and spatial data. **27**, 247–277 (2012).
45. Muggeo, V. M. R. Estimating regression models with unknown break-points. *Stat Med* **22**, 3055–3071 (2003).
46. Merchant, C. J. *et al.* Satellite-based time-series of sea-surface temperature since 1981 for climate applications. *Scientific Data* **6**, 223 (2019).

Supplementary Material

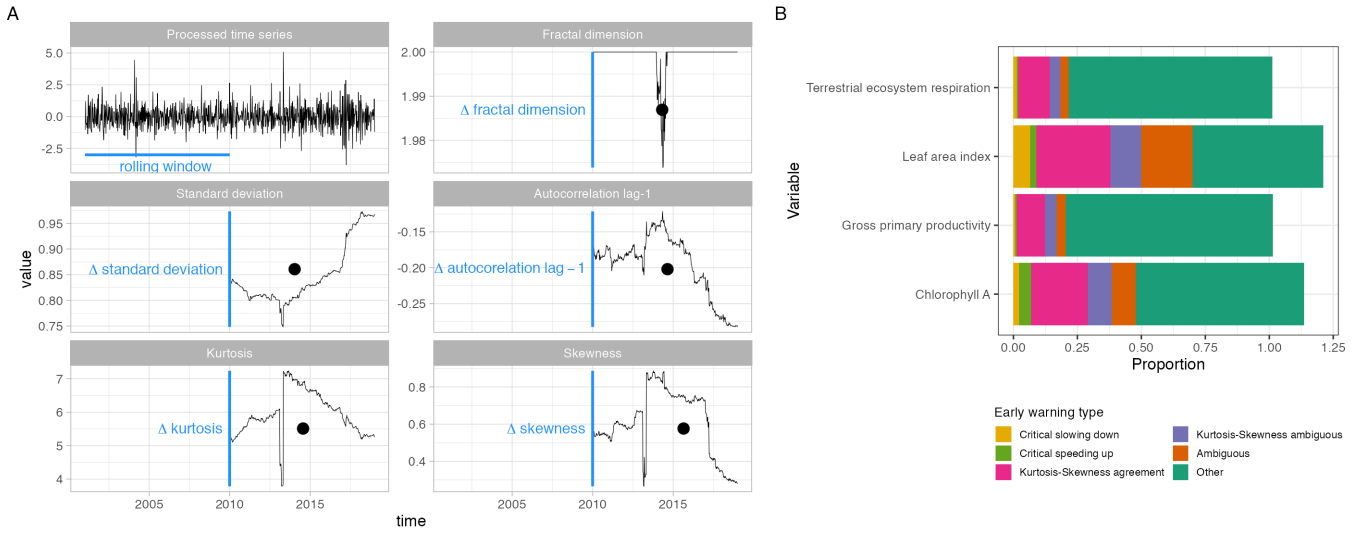


Figure S1: **Example with one pixel** Early warning signals for one pixel of the gross primary productivity dataset. A rolling window of half the length of the time series is used to calculate the dynamic indicators of resilience. Δ is the difference between maximum and minimum values, and the black points signal the break point of a segmented regression used to detect whether there are big jumps (increase or decrease) on the resilience indicators (A). (B) shows the coherence between resilience indicators across different datasets. The are labelled critical slowing down if both variance and autocorrelations increases, or speeding up if they decrease. If they contradict, they are labelled ambiguous. The same pixels can fill more than one early warning type, thus proportions can be > 1 .

A

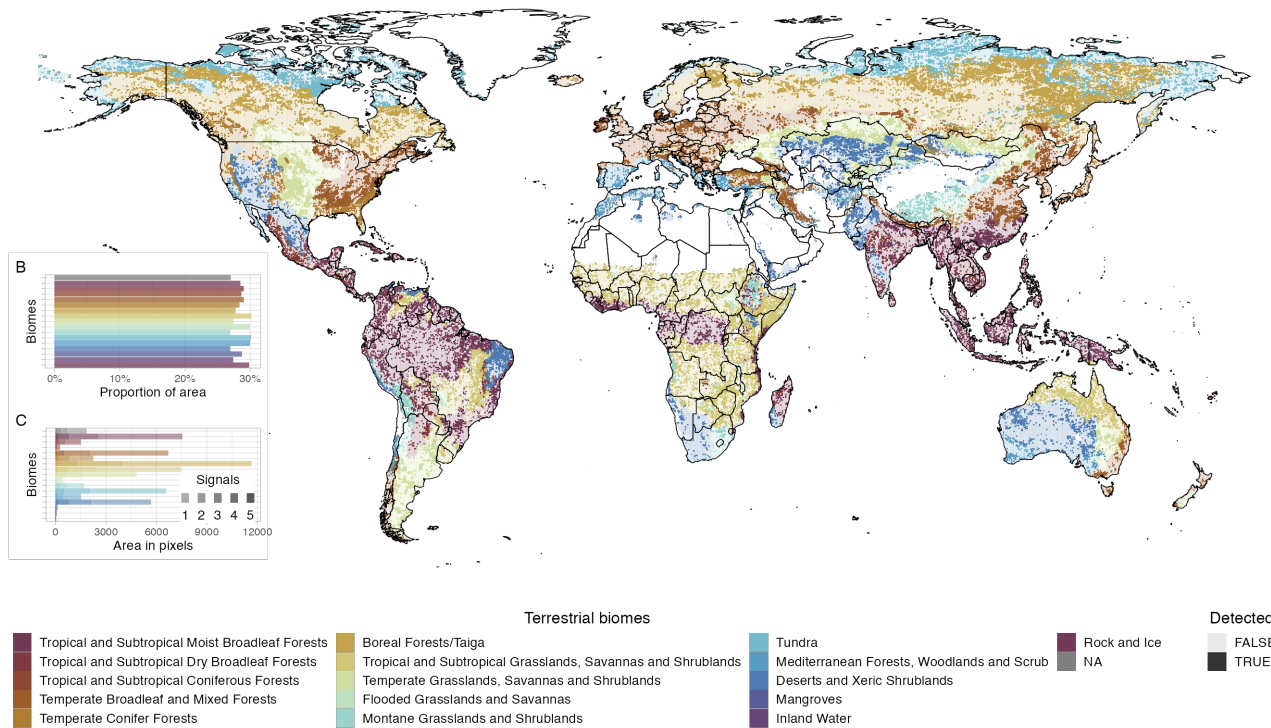


Figure S2: Terrestrial ecosystem respiration Detection of resilience loss in terrestrial biomes for terrestrial ecosystem respiration. A) shows where are biomes showing symptoms of resilience loss, B) aggregates proportion of area per biome, while C) shows area in 0.25 degree pixels.

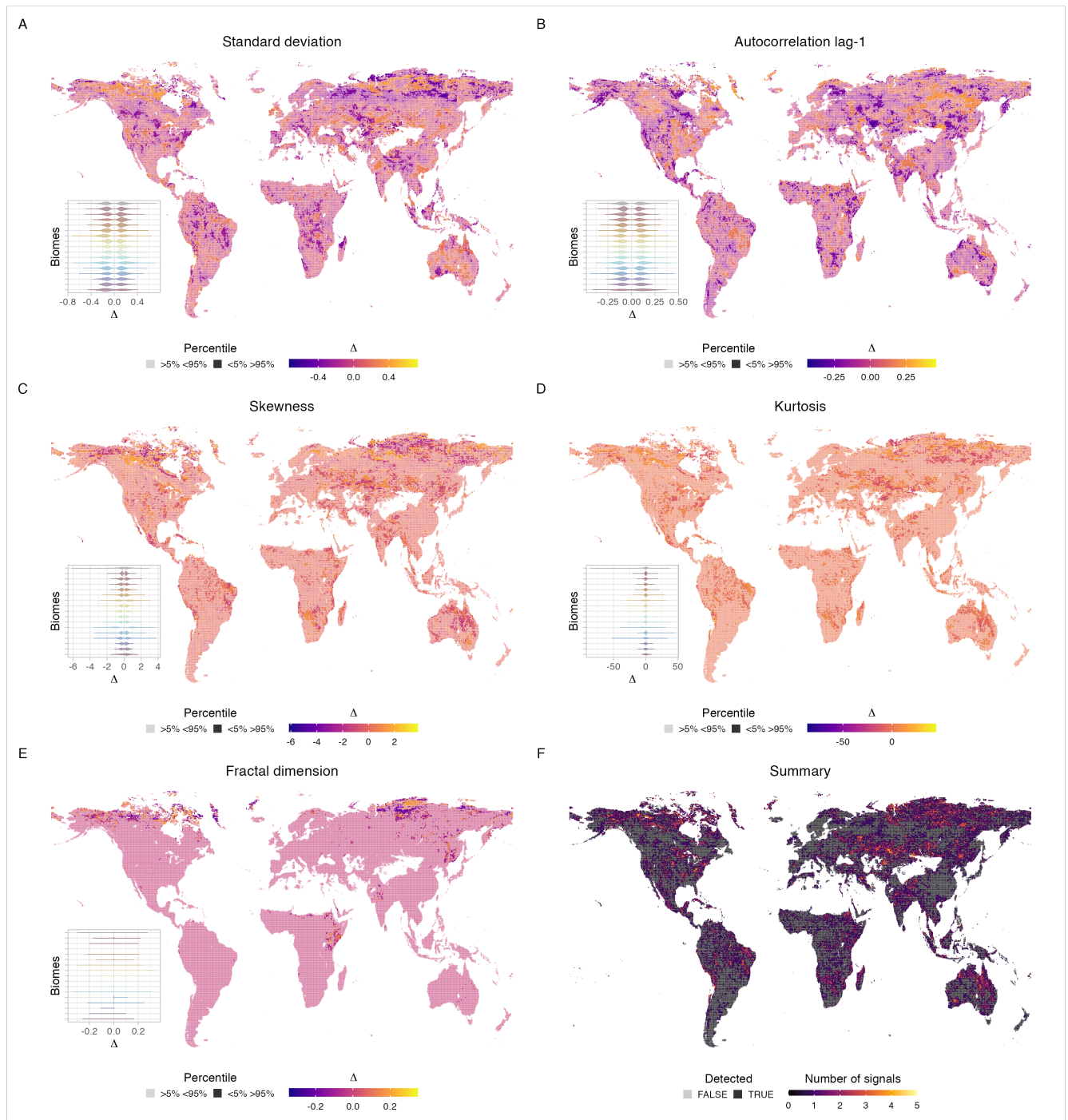


Figure S3: Resilience indicators in gross primary productivity Maps of the Δ outliers per biome are shown for standard deviation (A), autocorrelation at lag-1 (B), skewness (C), kurtosis (D), and fractal dimension (E). Insets show the distribution of Δ for each biome following the same colouring scheme of fig 1. (F) is the summary with the aggregated number of signals.

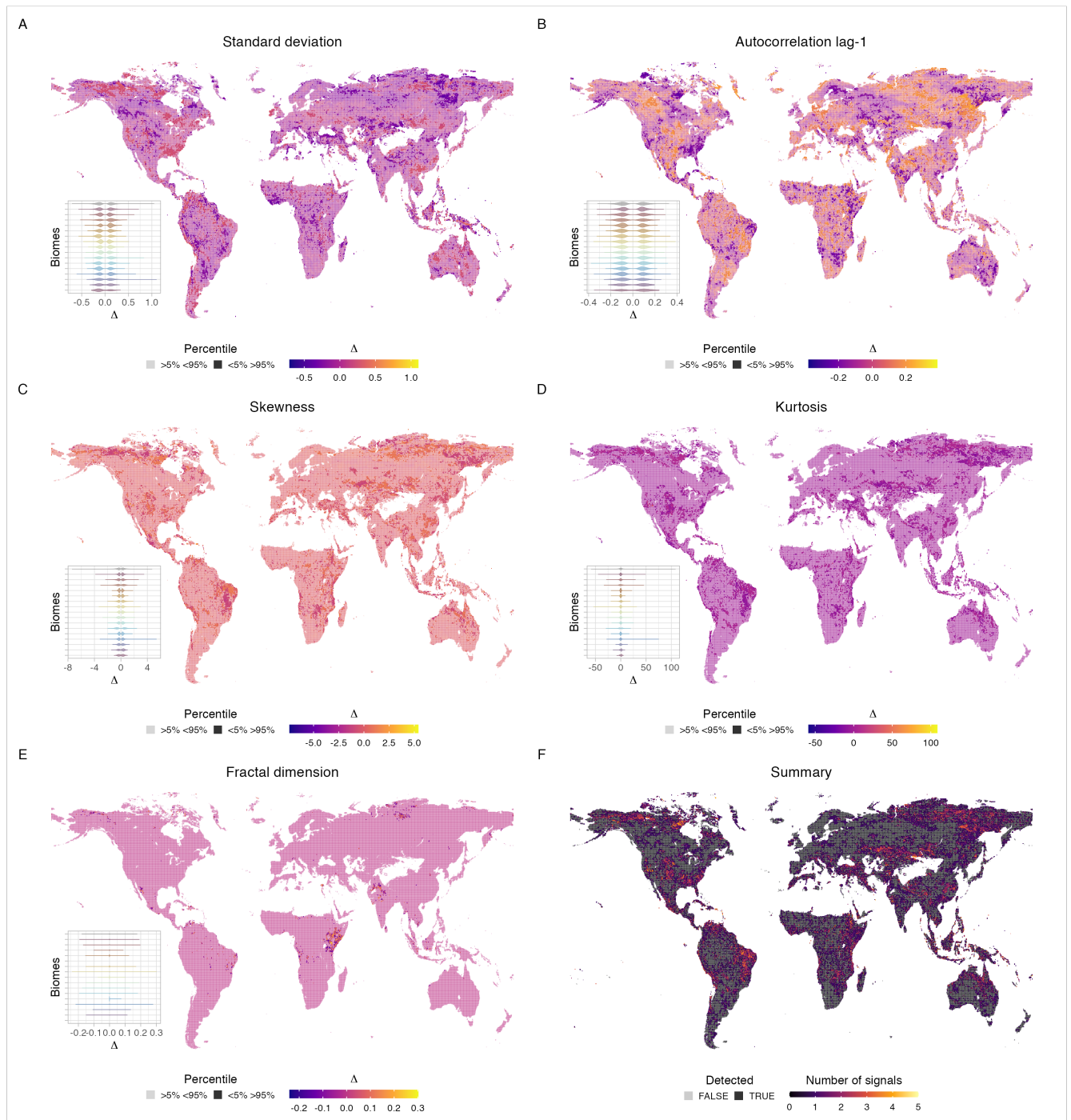


Figure S4: Resilience indicators in terrestrial ecosystem respiration Maps of the Δ outliers per biome are shown for standard deviation (A), autocorrelation at lag-1 (B), skewness (C), kurtosis (D), and fractal dimension (E). Insets show the distribution of Δ for each biome following the same colouring scheme of fig S2. (F) is the summary with the aggregated number of signals.

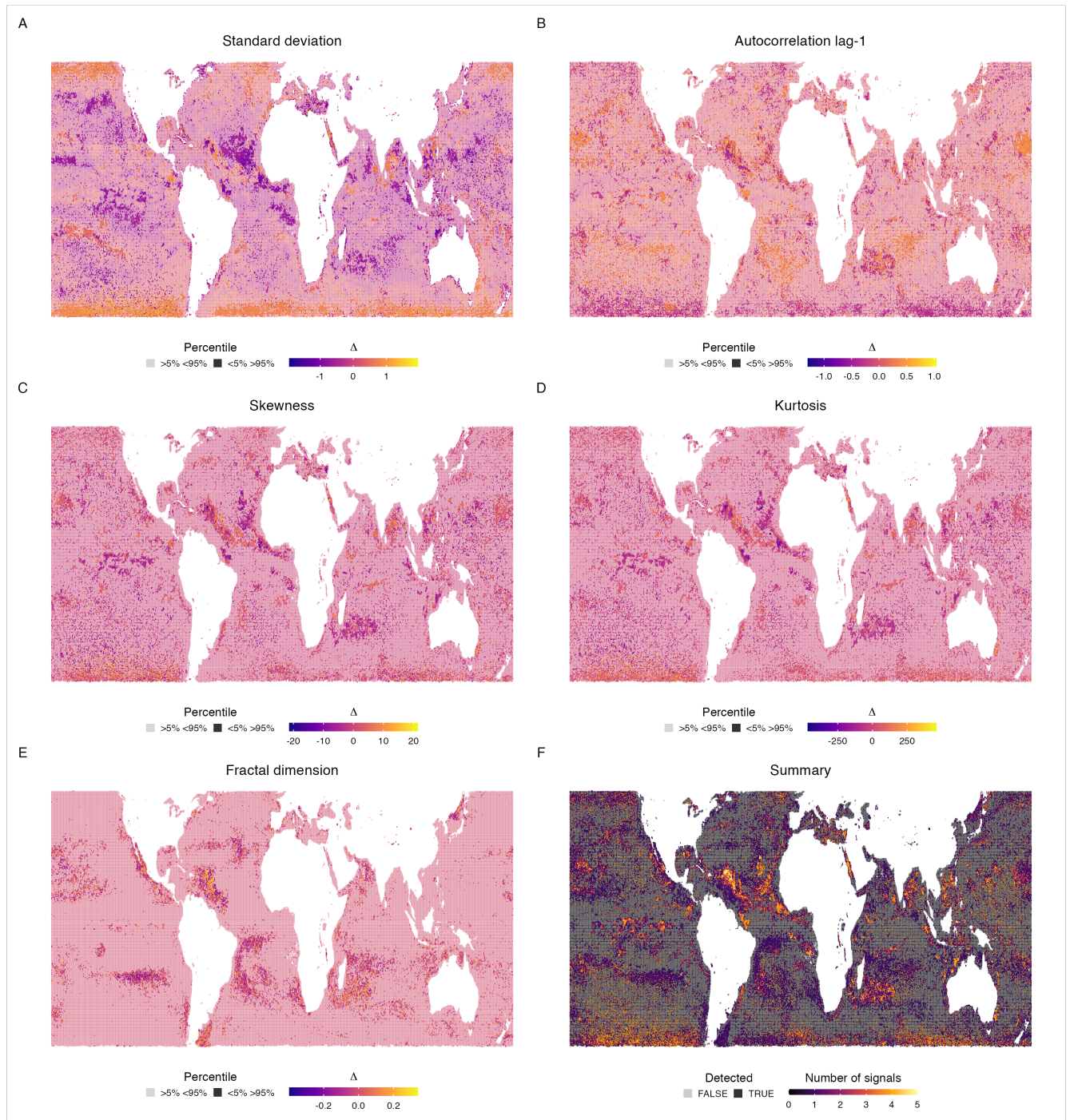


Figure S5: Resilience indicators in chlorophyll **A** Maps of the Δ outliers per biome are shown for standard deviation (A), autocorrelation at lag-1 (B), skewness (C), kurtosis (D), and fractal dimension (E). Insets show the distribution of Δ for each biome following the same colouring scheme of fig 2. (F) is the summary with the aggregated number of signals.

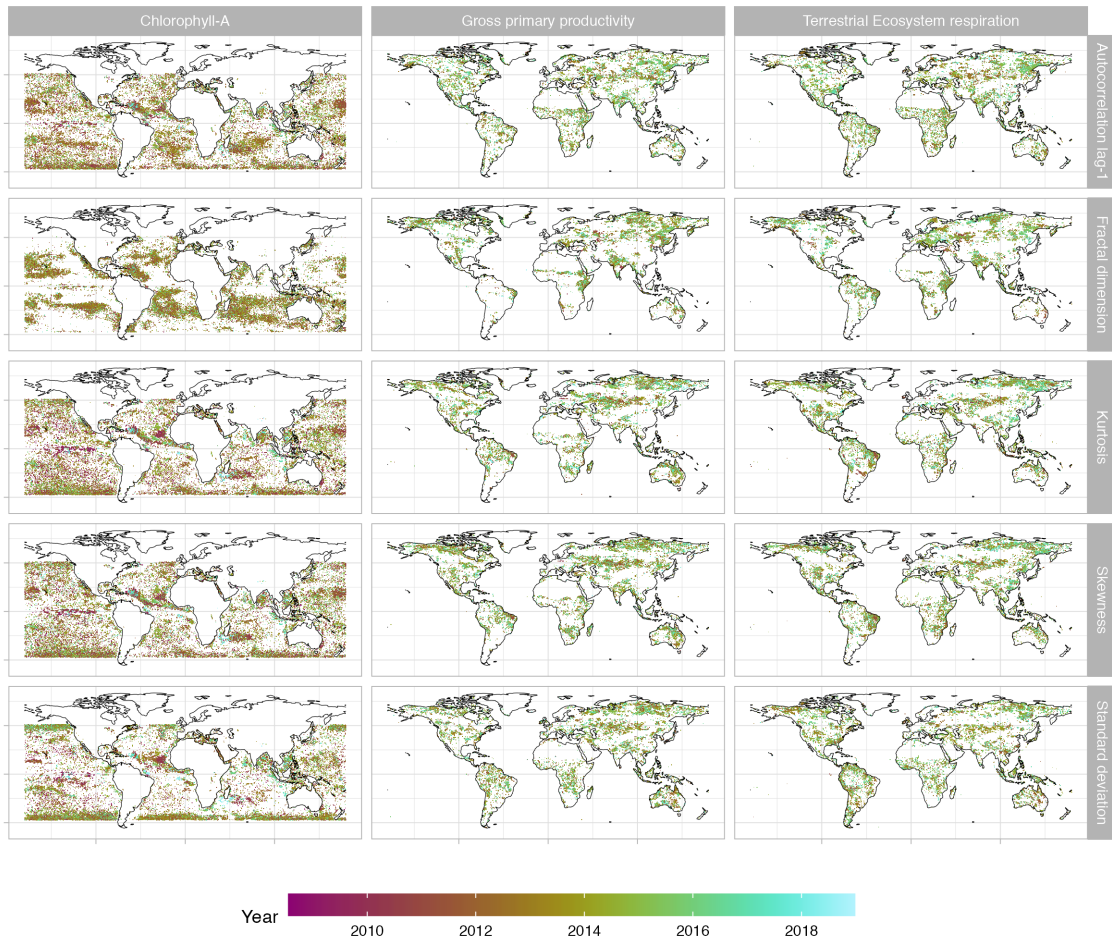


Figure S6: **Spatial and temporal coherence** Break points of the segmented regressions are show as maps for each dataset. The clustering in time and space of the dynamic indicators of resilience supports the idea that some areas are under similar pressures and can shift in tandem.

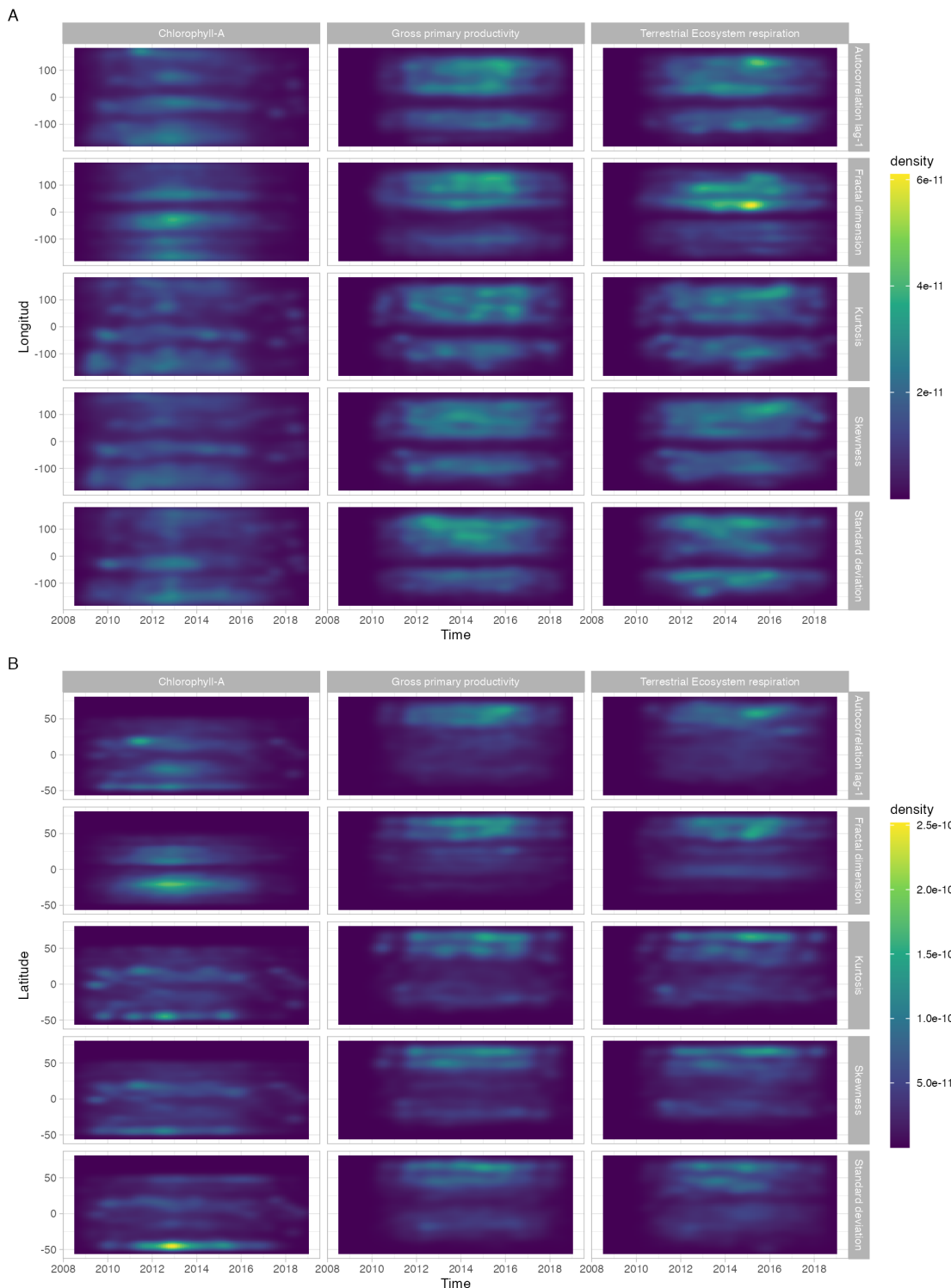


Figure S7: Temporal coherence of signals Probability density function of the location of break points in time and space for longitud (A) and latitud (B).

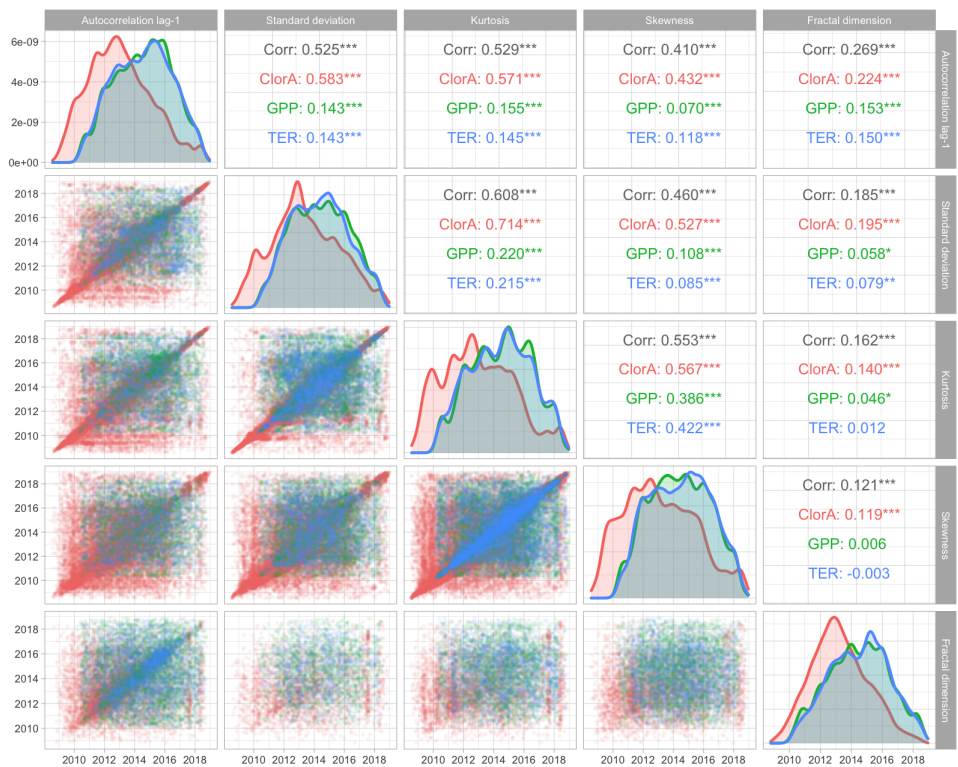
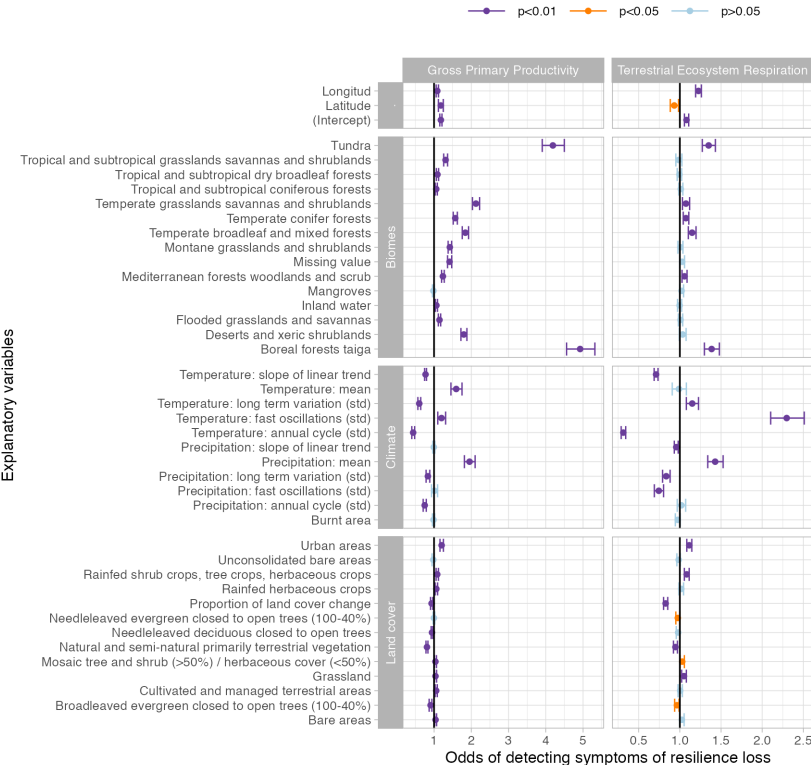
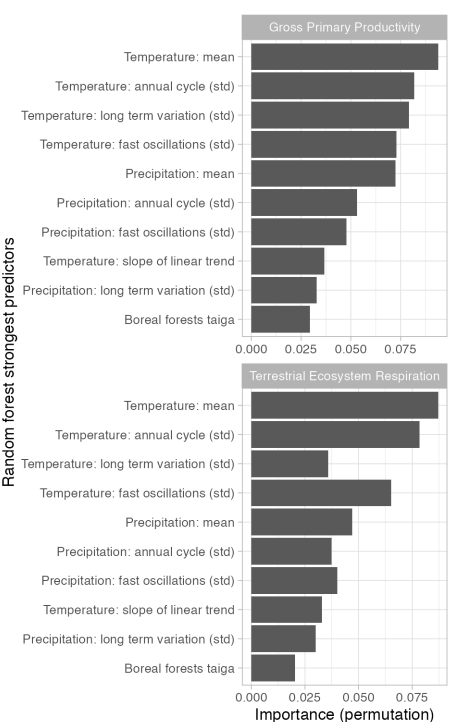


Figure S8: **Temporal correlations** Correlations in time of resilience indicators across datasets: gross primary productivity (GPP), terrestrial ecosystem respiration (TER), and chlorophyll A (ClorA)

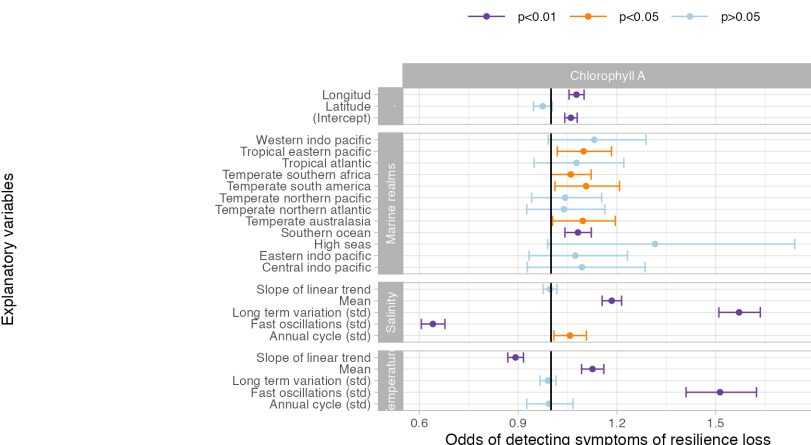
A



B



C



D

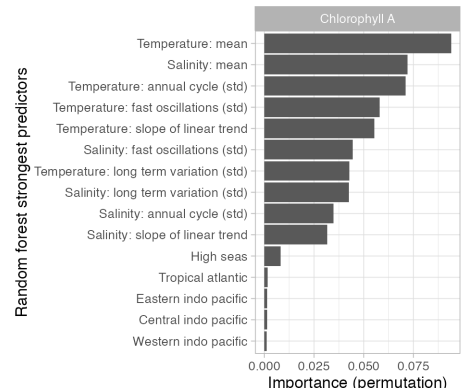


Figure S9: Predictors of resilience loss Logistic regressions to predict signals of resilience loss in gross primary productivity, terrestrial ecosystem respiration (A), and chlorophyll A (C). The strongest predictors of the random forest for terrestrial systems (B) and marine realms (D) were calculated with a permutation method. All random forest fitted 1000 trees. The best model for gross primary productivity targeted node size 10 and 12 variables to split at each node ($N = 31122$, OOB error 0.13), 20 node size and 9 variables for terrestrial ecosystem respiration ($N = 29546$, OOB error 0.14), and 20 node size and 9 variables for chlorophyll A ($N = 54298$, OOB error 0.16).

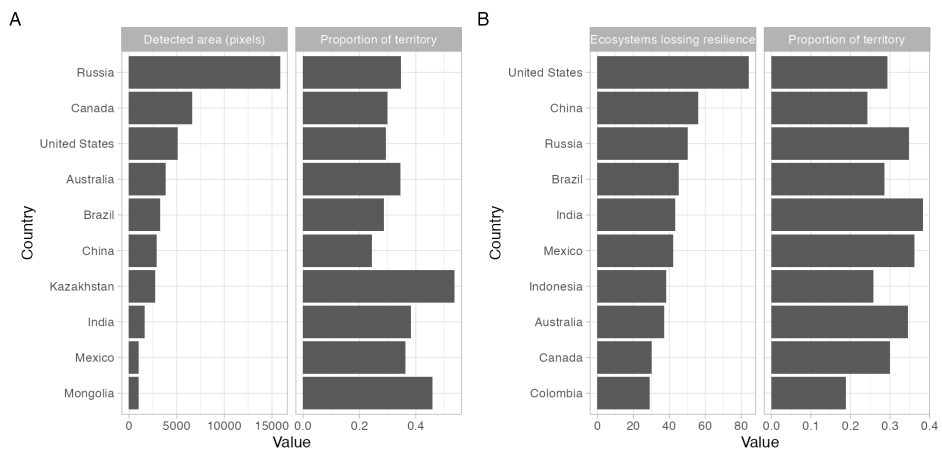


Figure S10: Most affected countries Top 10 countries by aggregated area in 0.25 degree pixels showing symptoms of resilience loss and as proportion of their territory (A). Countries ranked in (B) by the number of unique ecosystems showing symptoms of resilience loss and their proportion of territory impacted.